Noise induces spontaneous synchronous aperiodic activity in EI neural networks

Maria Marinaro and Silvia Scarpetta

Dipartimento di Fisica "E. R. Caianiello", Salerno University, Baronissi (SA), Italy
INFM, Sezione di Salerno, IT, and IIASS, Vietri sul mare (SA), Italy

Abstract. We analyze the effect of noise on spontaneous activity of a excitatory-inhibitory neural network model. Analytically different regimes can be distinguished depending on the network parameters. In one of the regimes noise induces synchronous aperiodic oscillatory activity in the isolated network (regime B). The Coherent Stochastic Resonance phenomena occur. Activity is highly spatially correlated (synchrony), it's oscillatory on short time scales and it decorrelates in time on long time scale (aperiodic). At zero noise the oscillatory activity vanishes in this regime. Changing parameters (for example increasing the excitatory-to-excitatory connection strength) we get spontaneous synchronous and periodic activity, even without noise (regime C). The model is in agreement with the measurements of spontaneous activity of two-dimensional cortical cell neural networks placed on multi-electrode arrays performed by Segev et.al [2].

1 Introduction and motivations

Recently much effort has been devoted to study in-vitro grown neural networks in isolation. In particular, Segev et al. [2] have done long term measurements of spontaneous activity of cortical cells neural network placed on multi-electrodes arrays. They observed both aperiodic synchronized bursting activity and periodic synchronized bursting activity, depending on values of Ca concentration. Some of their observations, and in particular some Power Spectrum Density (PSD) features, differ from the prediction of current computational neural network models and as far as we know, they have not been explained before. The aim of this paper is to show that a variant of the EI neural network model, introduced in a previous paper by one of us and collaborators [1] to model driven-activity and plasticity in cortical areas, is able to reproduce experimental results of spontaneous activity when we consider the model in isolation with intrinsic noise. Recently effects of noise on dynamics of various neural network models have been investigated in literature, using different thecniques like mean field theory, numerical simulations etc (see e.g. [3, 4] and references therein). Here analytical solution of the stochastic equations in the linear approximation are studied; then noise and nonlinearity effects are taken into account, both analytically and with numerical simulations. In sec 2 the model is described and in sec 3 the analytical and numerical results are reported together with comments and conclusions.

2 The model

The state variables u_i, v_i of the many interacting excitatory and inhibitory neurons evolve throw time, following the stochastic equations of motion:

$$\dot{u}_i = -\alpha u_i - \sum_j H_{ij} g_v(v_j) + \sum_j J_{ij} g_u(u_j) + \bar{F}_i(t), \tag{1}$$

$$\dot{v}_i = -\alpha v_i + \sum\nolimits_j W_{ij} g_u(u_j) + F_i(t). \tag{2}$$

where $g(u_i(t))$ is the instantaneous rate of spiking of the i^{th} neuron at time t, $i = 1 \ldots N$, α^{-1} is a time constant (about few milliseconds, for simplicity it is assumed equal for excitatory and inhibitory units), J_{ij}, W_{ij} and H_{ij} are the synaptic connection strengths. All these parameters are non-negative; the inhibitory character of the second term on the right-hand side of Eqn. (1) is indicated by the minus sign preceding it. $\bar{F}_i(t)$ and $F_i(t)$ model the intrinsic noise, respectively on the excitatory and inhibitory units, not included in the definition of u, v. In a (cultured) interacting neurons systems noise can be due to several reasons, like thermal fluctuation, ion channel stochastic activities, and many others. We take the noise $\bar{F}_i(t), F_i(t)$ to be uncorrelated white noise, such that $< F_i(t) >=< \bar{F}_i(t) >= 0$ and $< F_i(t) F_j(t') >=< \bar{F}_i(t) \bar{F}_j(t') >= \Gamma \delta_{ij} \delta_{t-t'}$. Note that even if the connection-matrices $\mathsf{J}, \mathsf{H}, \mathsf{W}$, are symmetric (plus random fluctuations), the connections between excitatory and inhibitory neurons are still highly asymmetric in this scenario, and the total connection matrix $\left(\begin{smallmatrix} \mathsf{J} & -\mathsf{H} \\ \mathsf{W} & 0 \end{smallmatrix}\right)$ is still asymmetric. An oscillatory state vector $\mathbf{u}(t) = \boldsymbol{\xi} cos(\omega_0 t) = \boldsymbol{\xi} e^{\mathrm{i}\omega_0 t} + \text{c.c.}$, where $\boldsymbol{\xi}$ have real positive-or-null elements correspond to a periodic synchronous bursting activity, and ξ_i describe the amplitudes of bursting on the different excitatory units. Then the local power spectrum density, PSD_i, and the global power spectrum, $PSD = 1/N \sum_i PSD_i$, will have a peak at $\omega = \omega_0$. We can describe both synchronous and phase-locked periodic activities cases by writing $u_i(t) = \xi_i e^{-\mathrm{i}\omega_0 t} + \text{c.c.}$, taking the ξ_i real in the first case and complex ($\xi_i = |\xi_i| e^{\mathrm{i}\phi_i}$) in the second.

3 Model analysis

Since the connectivity formation of the cultured system we want to model has grown randomly and spontaneously, we can reasonably assume that strength of each connection is a function only of the type of pre-synaptic and post-synaptic neurons (Excitatory or Inhibitory) and eventually of the distance between them (plus some random quenched fluctuations). In particular, since we are modelling cortical area, we will assume the W and J connections to be long range connections, $J_{ij} = \frac{j_0}{N}(1 + \epsilon \eta_{ij})$, $W_{ij} = \frac{W_0}{N}(1 + \epsilon \eta_{ij})$ and the inhibitory-to-inhibitory connections H to be local, $H_{ij} = h_0 \delta(i - j)(1 + \epsilon \eta_{ij})$, where $\epsilon << 1$ and η_{ij} is a random quenched value between -1 and 1. Therefore the three connection matrices have the common principal eigenvector $\boldsymbol{\xi}_0 = (1/\sqrt{N}, \ldots, 1/\sqrt{N})$ (apart from a correction of order $O(\epsilon/\sqrt{N})$), with eigenvalues j_0, W_0, h_0 respectively (with corrections $O(\epsilon/N)$). In the subspace orthogonal to the principal eigenvector the eigenvalues of J and W are negligible (of order ϵ/N). Here we take $\epsilon = 0$. Let's call $\{\bar{\mathbf{u}}, \bar{\mathbf{v}}\}$ the fixed point determined by $\dot{\mathbf{u}} = 0, \dot{\mathbf{v}} = 0$ with $\bar{\mathbf{F}}(t) = 0, \mathbf{F}(t) = 0$. Linearizing the equations (1,2) around the fixed point $\{\bar{\mathbf{u}}, \bar{\mathbf{v}}\}$, eliminating $\mathbf{v}$ from the equations, and assuming noise to be only on the $\mathbf{v}$ units, we obtain

$$\ddot{\mathbf{u}} + (2\alpha - \mathsf{J})\dot{\mathbf{u}} + [\alpha^2 - \alpha\mathsf{J} + \mathsf{HW})]\mathbf{u} = -\mathsf{H}\mathbf{F}(t) \tag{3}$$

where $\mathbf{u}$ is now measured from the fixed point value $\bar{\mathbf{u}}$, and nonlinearity enters only thou the redefinition of the elements of J H and W: $J_{ij}g'_u(\bar{u}_j) \to J_{ij}$, $H_{ij}g'_u(\bar{v}_j) \to H_{ij}$ and $W_{ij}g'_u(\bar{u}_j) \to W_{ij}$. We use bold and sans serif notation (e.g. $\mathbf{u}, \mathsf{J}$) for vectors and matrices respectively. The fixed point $(\bar{\mathbf{u}}, \bar{\mathbf{v}})$ is stable if the homogeneous associate equation of the Eq. (3) has only decaying solutions $\mathbf{u}$. In particular, when J, H and W share the same set of eigenvectors $\boldsymbol{\xi}_n$, denoting with j_n, W_n and h_n their eigenvalues, then eigensolutions are $\mathbf{u}_n = e^{\lambda_n t}\boldsymbol{\xi}_n + \text{c.c.}$, where

$$\lambda_n = -\frac{2\alpha - j_n}{2} \pm \frac{\sqrt{{j_n}^2 - 4h_n W_n}}{2} \tag{4}$$

and stability condition is $\text{Re}[\lambda_n] < 0$ i.e., the real parts $\text{Re}[\lambda_n]$ of the eigenvalues λ_n of the homogeneous system must be negative. Since the state vector $\mathbf{u}$ is a linear combination of all the eigenmodes, given by $\mathbf{u} = \sum_n c_n e^{\lambda_n t}\boldsymbol{\xi}_n + \text{c.c.}$ in the absence of noise $\Gamma = 0$, if all the n modes have $\lambda_n = \text{Re}[\lambda_n] < 0, (\text{Im}[\lambda_n] = 0)$, then the activity $\mathbf{u}$ simply decays toward the fixed point stationary state (regime A). However, if $\text{Re}[\lambda_n] < 0$ for each n, but $\exists n$ (call it $n = 0$) such that the imaginary part $\text{Im}[\lambda_0] \neq 0$, then, spontaneous collective aperiodic oscillations are induced by noise (regime B) as shown in the following section. Finally if $\text{Im}[\lambda_0] \neq 0$ and $\text{Re}[\lambda_0] > 0$ we get the regime C that will be analyzed in sec 3.2.

3.1 Regime B: Coherent Stochastic resonance phenomena

Let's analyze the dynamics of the stochastic system (3), when $\text{Re}[\lambda_n] < 0$ for each n and $\text{Im}[\lambda_n] = 0$ except for n=0. The state vector $\mathbf{u}$ is a linear combination of all the eigenmodes $\mathbf{u} = \sum_n (m_n(t) + \text{c.c.})\boldsymbol{\xi}_n$, in particular, when $\lambda_0 = -1/\tau_0 \pm \mathrm{i}\omega_0$, it is

$$m_0(t) = [a_0 cos(\omega_0 t) + b_0 sin(\omega_0 t)]e^{-t/\tau_0} + \frac{1}{\omega_0}\int_0^t ds\ e^{-(t-s)/\tau_0}\ sin(\omega_0(t-s))\ F_0(s) \tag{5}$$

where $F_0(s)$ is the projection of the noisy term $-\mathsf{H}\mathbf{F}$ on the eigenvector $\boldsymbol{\xi}_0$, and $< F_0(s)F_0(s') >= h_0^2 \Gamma \delta(s - s')$. The correlation function of excitatory unit i, $\langle u_i(t)u_i(t')\rangle - \langle u_i(t)\rangle\langle u_i(t)\rangle = C_i(t - t')$ and the global correlation function $C(t-t')$ are the sum of the contributions of each mode, in particular $C(t-t') = \sum_i C_i(t-t') = \sum_n \langle (m_n + \text{c.c.})(m_n + \text{c.c.})\rangle - \sum_n \langle (m_n + \text{c.c.})\rangle\langle (m_n + \text{c.c.})\rangle \equiv \sum_n C^n(t-t')$. The PSD, i.e. the Fourier Transform $\tilde{C}(\omega)$, is just the sum of the n contributions: if λ_n is real, $\lambda_n = -1/\tau_n < 0$, then its contribution to the PSD is just

$$\tilde{C}^n(\omega) \propto \frac{h_0^2 \Gamma \tau_n^4}{(1 + \omega^2\tau_n^2)^2} \tag{6}$$

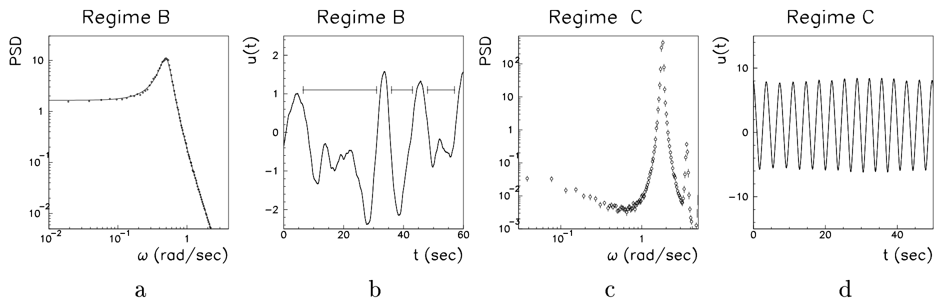

Fig. 1. a. Power Spectrum Density of excitatory units, of the linear system in the regime B, with $\Gamma = 0.0004$. Dots are numerical simulations results while solid line is our theoretical prediction. We use the following parameters: $N = 10$, $\alpha = 50 sec^{-1}$, $J_{ij} = \frac{j_0}{N} = 9.98$ sec^{-1}, $W_{ij} = W_0/N, H_{ij} = h_0\delta(i-j)$, and $W_0 = h_0 = \sqrt{(j_0/2)^2 + 0.5^2} = 49.9 sec^{-1}$, so that $\omega_0 = 0.5 rad/sec$. b. The time behavior of the state variable $u_i(t), i = 1, \ldots, 10$ of linear system in the regime B, with $\Gamma = 0.004$. All units $u_i(t)$ shows synchronous oscillatory activity. Differences in the activity between the state variables $u_i(t)$ are so small that all the lines $u_i(t)$ overlaps each other. c. Power Spectrum Density of excitatory units in regime C with $\Gamma = 0.0004$, using the saturating activation function shown in Fig. 2.A in dashed red line. In particular, $N = 10$, $\alpha = 50 sec^{-1}$, $J_{ij} = \frac{j_0}{N} = 10.014$, $W_0 = h_0 = 50.07$, so that $\omega_0 = 0.5 rad/sec$ and oscillation frequency is $\omega = 1.9 rad/sec$ following eq. (11). d. State variable $u_i(t), i = 1, \ldots, 10$ versus time in the regime C, with $\Gamma = 0.004$. All units $u_i(t)$ shows synchronous oscillatory periodic activity.

peaked at $\omega = 0$, however if $\mathrm{Im}[\lambda_0] = \omega_0 \neq 0$ and $\mathrm{Re}[\lambda_0] = -1/\tau_0 < 0$, its contribution to the time correlation is

$$C^0(t-t') = h_0^2 \Gamma \frac{\tau_0^3}{4(1+\omega_0^2\tau_0^2)} e^{-|t-t'|/\tau_0} [cos(\omega_0|t-t'|) + \frac{1}{\omega_0\tau_0} sin(\omega_0|t-t'|)] \quad (7)$$

and the contribution to the PSD is

$$\tilde{C}^0(\omega) = h_0^2 \Gamma \frac{\tau_0^4}{4(1+\omega_0^2\tau_0^2)} [\frac{2+\omega/\omega_0}{1+\tau_0^2(\omega+\omega_0)^2} + \frac{2-\omega/\omega_0}{1+\tau_0^2(\omega-\omega_0)^2}] \quad (8)$$

peaked at ω close to ω_0 (if $\frac{1}{\tau_0} > \omega_0$). Therefore the linear analysis predict that noise induces a collective oscillatory behavior in the neurons activity, in the parameter region when $\lambda_0 = -1/\tau_0 \pm i\omega_0$ (and $\frac{1}{\tau_0} > \omega_0$). This collective oscillatory behavior correspond to a broad peak in the power-spectrum of the neurons activity close to the characteristic frequency ω_0. Numerical simulation results are shown in Fig.1.ab Oscillations are synchronous because $\boldsymbol{\xi}_0$ has real positive elements. The signal looks aperiodic on long time scale, since the noise decorrelates over long time scale the signal. This spontaneous aperiodic synchronous activity mimic the spontaneous aperiodic synchronous activity observed under 0.5 and 2.0 mM Ca concentration in [2]. Effects of nonlinearity and noise in this regime

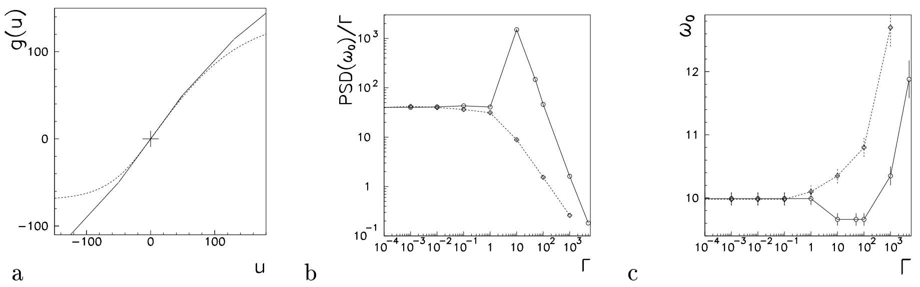

a b c

Fig. 2. a. Two activation functions for excitatory units u_i. Dashed line shows a saturating activation function (used in most of the following simulations), while solid line shows a piece-wise-linear function, whose slope increases before decreasing when u is raised from its stationary value (cross). b. Ratio $R = PSD(\omega_0)/\Gamma$ as a function of the noise level Γ. Dashed line correspond to the saturating activation function shown in A, while the solid line to the solid line activation function in A. We used the following parameters in the simulations: $N = 10$, $\alpha = 50sec^{-1}$ $J_{ij} = \frac{j_0}{N} = 9.98sec^{-1}$, $W_0 = h_0 = 50.89sec^{-1}$, so that $\omega_0 = 10rad/sec$. c. The frequency of the PSD peak versus the noise level (same simulations as in B). Effect of nonlinearity is evident in both fig. b and c, indeed for linear system R and ω_0 do not change with noise level.

B have being investigated numerically. Fig. 2.b shows the ratio $R = \tilde{C}(\omega_0)/\Gamma$ between the output power at th peak close to the characteristic frequency ω_0 and the power of the noise Γ, versus the noise level, using two different activation functions. The first activation function deviates from linearity near the fixed point due to saturation (red dashed line), while in the second (black solid line) the slope increase before decreasing when the u is raised from its stationary value. Solid line in Fig. 2.b shows the typical maximum that has become the fingerprint of *Stochastic Resonance* phenomena. Fig. 2.c shows that oscillation frequency change slowly with the noise level Γ. If the excitatory-to-excitatory connections are more strong so that $\mathrm{Re}[\lambda_{n=0}] = \alpha - j_0/2 \geq 0$, but not too much strong so that it is still $\mathrm{Im}[\lambda_0] \neq 0$, then interesting spontaneous activity arise also without noise. In particular, spontaneous periodic oscillations arise in the linear approximation if $\mathrm{Re}[\lambda_0] = 0$ and $\mathrm{Im}[\lambda_0] \neq 0$, this is a critical point separating the regimes $\mathrm{Re}[\lambda_0] < 0, \mathrm{Im}[\lambda_0] \neq 0$ (regime B) and $\mathrm{Re}[\lambda_0] > 0, \mathrm{Im}[\lambda_0] \neq 0$ (regime C).

3.2 Regime C: Spontaneous synchronous periodic activity

In the regime C linear analysis predict synchronous periodic activity with diverging amplitude, that become stable when nonlinearity is taken into account.

Eliminating $\mathbf{v}$ from equation (1) and (2), we have the non-linear differential equation (analog to the linear eq.(3)),

$$[(\alpha + \partial_t)^2]\mathbf{u} - [(\partial_t + \alpha)\mathsf{J} - \mathsf{HW}]g_u(\mathbf{u}) = -\mathsf{H}\mathbf{F}(t) \tag{9}$$

where u_i is measured from the fixed point value $\bar{u}_i$, $g_u(\mathbf{u})$ means a vector with components $[g_u(\mathbf{u})]_i = g_u(u_i)$, and we take for simplicity g_v as linear. Let's analyze the case when g_u deviates from linearity near the fixed point $\bar{\mathbf{u}}$ due to saturation: $g_u(u_i) \sim u_i - au_i^3$ where $a > 0$. This case includes most standard sigmoids used in modeling, including logistic sigmoids, hyperbolic tangent and the function marked by red dashed line in Fig. 2.A that we used in our numerical simulations. We look self-consistently for solutions like $\mathbf{u} = q\boldsymbol{\xi}_0 e^{-\mathrm{i}\omega t} + \mathrm{c.c.}+$ higher order harmonics, where $\boldsymbol{\xi}_0$ is the spatial pattern corresponding to the principal eigenvector of the connection matrices, and q is a macroscopic variable (the order parameter) measuring how much the system activity is similar to the periodic oscillating activity of interest. Our calculations predict that periodic synchronous oscillations ($q \neq 0$) arise only when the excitatory-to-excitatory strength is in the proper range

$$2\alpha < j_0 < 2(h_0 W_0)/\alpha \tag{10}$$

with both an upper and lower limit, and that the oscillation frequency is given (self-consistently) by

$$\omega^2 = 2h_0 W_0 \alpha / j_0 - \alpha^2. \tag{11}$$

Since the extracellular Ca is known to affect the synapse probability of neurotransmitter release, the analytical prediction (10) can explain why only for a critical interval of concentrations of Ca2+ the periodic synchronous oscillations has been observed in cultured neural networks (it arise at $\sim 1mM$, not at *lower* or *higher* concentrations [2]). We have performed numerical simulations using the nonlinear saturating function shown in Fig. 2.a (dashed line). The noiseless nonlinear numerical simulations shows stable synchronous periodic spontaneous activity $\mathbf{u}$, with frequency in agreement with the nonlinear analysis predictions of eq. (11) (results not shown). Fig.1.cd shows simulation results with noise $\Gamma = 0.0004$, the two high peaks at first and second harmonic in the PSD and the broad band at low frequency (indicating positive long-term time correlations) mimic the experimental results of [2].

References

1. S. Scarpetta, Z. Li, J. Hertz. NIPS 2000. Vol 13. T. Leen, T. Dietterich, V. Tresp (eds), MIT Press (2001).
2. R. Segev, Y. Shapira, M. Benveniste, E. Ben-Jacob. Phys. Rev. E **64** 011920, 2001. R. Segev, M. Benveniste, E. Hulata, N. Cihen, A. Palevski, E. Kapon, Y. Shapira. Phys. Rev. Lett. 2002 (in press).
3. N. Brunel Jour. of Comp. Neurosc. 8, 183-208, 2000. N. Brunel FS. Chance, N. Fourcaud, LF. Abbot , Phys. Rev. E, 86 (10), p.2186-9, 2001
4. P.C. Bressloff , Phys. Rev. E, 60,2, 1999. Y. Shim, H. Hong, M.Y. Choi, Phys. Rev. E, 65, p.36114, 2002.